on-axis portion of the beam were made with the FROG technique after an 85-fs near-Gaussian pulse (with varying peak power) had traversed 3 cm of fused silica. The corresponding numerical simulations involve the solution of a modified 4-D nonlinear Schrödinger equation that accounts for linear and nonlinear shock effects, a Raman nonlinearity, and higher-order dispersion.[5]

As seen in Figure 1a, at the lowest power the input pulse has split into two sub-pulses, with the leading pulse being larger. The asymmetry of the splitting is primarily the result of the linear and nonlinear shock terms, and the predominant negative curvature of the phase (dashed line) indicates that the spectrum of the leading pulse is red-shifted with respect to the trailing pulse. At higher powers (Figs. 1b and 1c), we see further splitting to three pulses and then a coalescence of the multiple peaks toward a broader single pulse. All measurements are in good agreement with the theoretical predictions shown in Figures 1d–f. A more complete understanding of femtosecond propagation dynamics, as demonstrated by this work, should prove valuable to emerging applications that use femtosecond pulses in areas as diverse as optical communications, biological imaging, plasma physics, nonlinear frequency conversion, and remote sensing.

## References

1. D. Strickland and P.B. Corkum, "Resistance of short pulses to self-focusing," J. Opt. Soc. Am. B **11,** 492–497 (1994).
2. J.K. Ranka *et al.*, "Observation of pulse splitting in nonlinear dispersive media," Phys. Rev. Lett. **77,** 3783–3786 (1996).
3. R. Trebino *et al.*, "Measuring ultrashort laser pulses in the time-frequency domain using frequency-resolved optical gating," Rev. Sci. Inst. **68,** 3277–3295 (1997).
4. S.A. Diddams *et al.*, "Amplitude and phase measurements of femtosecond pulse splitting in nonlinear dispersive media," Opt. Lett. **23,** 379–381 (1998).
5. A.A. Zozulya *et al.*, "Investigations of nonlinear femtosecond pulse propagation with the inclusion of Raman, shock, and third-order phase effects," Phys. Rev. A **58,** 3303–3310 (1998).

## Long Distance Propagation in Air Due to Dynamic Spatial Replenishment

M. Mlejnek, E.M. Wright, and J.V. Moloney, Arizona Center for Mathematical Sciences, and Optical Sciences Center, Univ. of Arizona, Tucson, AZ.

Recently, there has been considerable excitement regarding experimental demonstrations of propagation of femtosecond pulses over $10^2$–$10^4$ m in air[1–4] due to its potential applications, *e.g.*, lightning channeling[2] and LIDAR.[3] To determine the utility of this phenomenon for these and other applications the underlying physics needs clarifying. The critical power for self-focusing in air is $P_{cr}$ = 1.7 GW. Catastrophic collapse is avoided by a combination of multi-photon ionization (MPI), and absorption and defocusing by the electron-plasma generated by MPI. Our question is: How do these mechanisms conspire to produce long distance propagation?

To address this issue we have performed numerical simulations using a comprehensive air propagation model.[5] Typical results for a 780-nm pulse of duration 200 fs (FWHM) and peak power $P_0$ = 10 GW are shown in Figure 1. The surface plots show intensity versus time (in a frame moving at the group velocity) and transverse dimension $x$ for various propagation distances $z$. The insets show the maximum on-axis intensity. The top plot for $z$ = 61 cm is close to the paraxial collapse distance, but MPI and plasma defocusing arrest the collapse yielding a stabilized pulse. This creates the impression that long distance propagation is due to the stabilization of collapse by MPI and plasma defocusing.[1] However, upon further propagation this pulse decays due to absorption, but the fascinating result is that a new pulse grows from the trailing edge pulse: This phenomenon is shown in the middle plot for $z$ = 148 cm where the leading edge pulse is decaying as the trailing edge pulse is growing. The formation of the trailing pulse is due to the re-self-focusing of the power that was displaced into spatial rings by the plasma-defocusing imposed on the trailing edge of the incident pulse by the collapsing front edge. In the bottom plot for $z$ = 161 cm the trailing edge pulse has now replaced the leading one.

This process that we term dynamic spatial replenishment, in which the initial pulse forms, is absorbed, and is

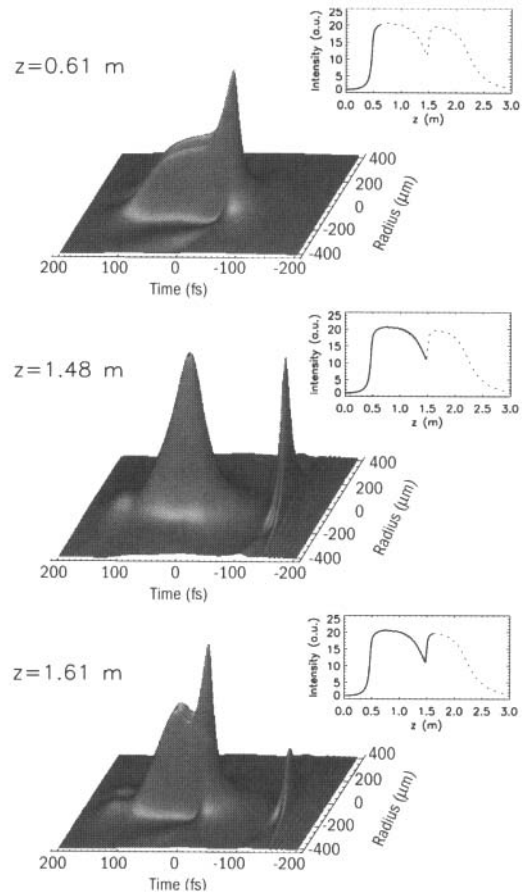


**Mlejnek Figure 1.** *The surface plots show intensity versus time* (in a frame moving at the group velocity) and transverse dimension $x$ for propagation distances $z$ = 61 cm (top), $z$ = 148 cm (middle), and $z$ = 161 cm (bottom). The solid line in each inset shows the maximum on-axis intensity up to that distance; the dashed line shows the intensity over the full range. The simulations were performed using the air parameters from Ref. 5, a laser wavelength of 780 nm, pulse duration 200 fs (FWHM), and a peak power $P_0$ = 10 GW. An input spot size of $\omega_0$ = 0.7 mm was used so that numerical simulations could be performed on the scale of 1 m, but the distance for larger spot sizes scales as $\omega_0^2$.

replenished by refocusing of the trailing edge, can occur several times for high-peak-power incident pulses and create the illusion of a single pulse propagating over a long distance. For experiments in which only the fluence is monitored, time integration masks the dynamics and creates the impression of one stabilized light filament. However, our simulations[5] show that the situation is more dynamic, and Brodeur *et al.*,[4] have presented experimental evidence of this.

### References

1. A. Braun *et al.*, "Self-channeling of high-peak-power femtosecond laser pulses in air," Opt. Lett. **20,** 73–75 (1995).
2. X.M. Zhao *et al.*, "Femtosecond ultraviolet laser pulse induced lightning discharges in gases," IEEE J. Quantum Electr. **31,** 599–612 (1995).
3. L. Woeste *et al.*, "Femtosecond atmospheric lamp," Laser und Optoelektronik **29,** 51–53 (1997).
4. A. Brodeur *et al.*, "Moving focus in the propagation of ultrashort laser pulses in air," Opt. Lett. **22,** 304–306 (1997).
5. M. Mlejnek *et al.*, "Dynamic spatial replenishment of femtosecond pulses propagating in air," Opt. Lett. **23,** 382–384 (1998).

## Seeking for New Propagation Invariant Wave-fields

Rafael Piestun, Dept. of Electrical Engin., Technion, Israel Institute of Technology, Haifa, Israel and Ginzton Lab., Stanford Univ., Stanford, CA; Joseph Shamir, Dept. of Electrical Engin., Technion, Israel Institute of Technology, Haifa, Israel.

The possibility of producing wave-fields (WFs) with propagation-invariant characteristics has generated wide interest in recent years.[1–6] These WFs are attractive for applications such as delivery of information and energy, beam shaping, atom guiding, interferometry, and measurements. Apart from the technological interest, the physical phenomena associated with such WFs provides insight into the ways to control and use diffraction.

The self-imaging (SI) WFs are a well-known example of periodic invariance, characterized by a repetition of the transverse field distribution. Another important class of propagation invariant (PI) WFs contains the so-called nondiffracting beams,[1] which keep a constant transverse intensity distribution. The existence of much wider classes of PI fields has recently been demonstrated.[2–6] Different extensions of the concept are obtained by relaxing the required conditions on the field, allowing, for example, different degrees of coherence,[2] or changes in scale[5] and orientation.[6] Such degrees of freedom, considered in the definition of invariance, lead to important new physical properties of the resulting WFs.

In Reference 6 we proposed a generalized concept of propagation-invariance applied to stationary fields satisfying the homogeneous Helmholtz equation. The introduced WFs present transverse field distributions that are exactly reproduced upon propagation, although not necessarily with the same azimuthal orientation.

We proved necessary and sufficient conditions stating that generalized PI WFs are composed of a discrete superposition of Bessel modes

$$U^{PI}(\rho,\varphi,z)=\sum_{mn}C_{mn}J_m(\alpha_{mn}\rho)\exp\left[i(\beta_{mn}z+m\varphi)\right] \qquad (1)$$

where $(\rho, \varphi, z)$ are cylindrical coordinates, $C_{mn}$ constants, $\alpha_{mn}=(k^2-\beta_{mn}^2)^{1/2}$, and

$$\beta_{mn}=\beta_0+(m\gamma+2\pi n)/\Delta z \qquad 0\le\beta_{mn}\le k$$

with $\gamma$ the azimuthal change in orientation of the transverse field, $\beta_0$ a constant, $k=2\pi/\lambda$, and $\Delta z$ the distance between transverse planes.

The fact that these conditions are necessary and sufficient implies that all possible PI WFs satisfying our criteria are described by Eq. 1. Another important outcome is that the transverse field distribution is periodically self-reproduced along $z$, in general, at different azimuthal positions.

Within this general class of PI WFs we can distinguish various interesting special cases, including the classical SI WFs and nondiffracting beams. First we uncovered a complete class of rotating WFs that present a constant transverse field distribution that continuously rotates along and about the propagation axis. In addition, we proved the existence of WFs with transverse distributions that are periodically reproduced with different azimuthal orientations. In this case, the transverse distribution is not necessarily constant as in the rotating WFs. A striking subclass is characterized by aperiodic rotated self-images, in the sense that they never return to their original orientation along the propagation (see Fig. 1a). Note that periodicity was long believed to be a necessary condition for exact self-reproduction of the field on propagation.

To understand the current generalization, we present the diagram of Figure 1b. The aperiodic rotated SI WFs constitute a completely new class, while the periodic rotated SI WFs and the rotating WFs are special cases of the classical SI effect. This fact was not apparent from the classical conditions defined for SI. The extent of the present generalization can be appreciated by consider-

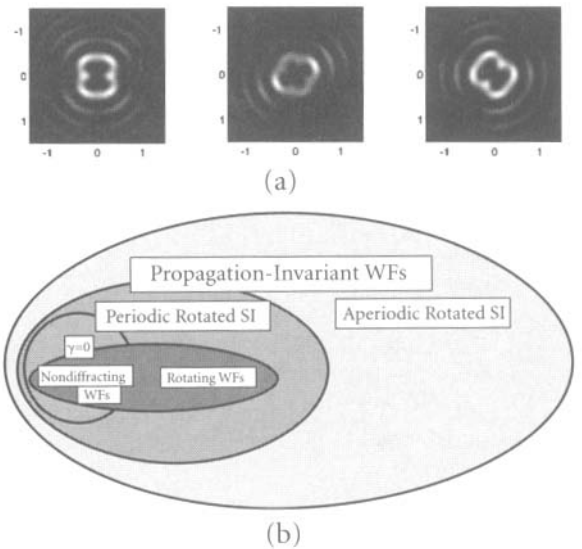


**Piestun Figure 1.** (a) Example of an aperiodic self-imaging WF: The transverse field is reproduced at different orientations, but never returns to its original state. Note the change in the field at intermediate planes. From left to right, $z=0$, $\Delta z/2$, $\Delta z$; $\gamma=52°$. All the units are microns. (b) Schematic of the relation among the different PI WFs.